Characterization of Sol-Gel Derived $CuO@SiO_2$ Nano Catalysts towards Gas Phase Reactions

Homaunmir, Vahidah
Islamic Azad University, Rasht Branch, Rasht, I.R. IRAN

Tohidi, Sayed Hossein*[+]
Agricaltur & Medical & Industrial Research School, Nuclear Science and Technology Institute, P. O. Box: 31485- 498, Karaj a, I.R. IRAN

Grigoryan, Garnik
Yerevan State University, 1 Alex Manoukian St., Yerevan 375049, ARMENIA

ABSTRACT: *One distinct concentration of copper ions was embedded into the silica matrix to xerogel form using copper source $Cu(NO_3)_2{\cdot}3H_2O$. The xerogel samples were prepared with using hydrolysis and condensation reactions of TetraEthyl Ortho-Silicate (TEOS) by the sol-gel method. In this investigation, new molar ratio of H_2O/TEOS was determined to be 11.7. Also, the necessary amount of tri-hydrated copper nitrate was added to the solution in such a manner that the concentration of the copper oxide in final solution reach to 10 wt. %. The prepared samples were characterized by Thermal Gravimetric Analysis (TGA), Transmission Electron Microscopy (TEM), surface area measurement (using BET method) and Thermal Program Reduction (TPR) methods. Finally, catalytic behavior of nano-composites was studied towards carbon monoxide (CO), nitrogen monoxide (NO) oxidation and di-nitrogen oxide (N_2O) decomposition reactions. The results were presented the systematic reactivity study of CO, NO oxidation and N_2O decomposition on dispersed copper oxide nano-catalysts over silica supports, in order to determine the ability of these materials to convert carbon monoxide, nitrogen monoxide and di-nitrogen oxide to harmless species by different reaction paths at different temperatures.*

KEY WORDS: *Copper oxide, Nano-catalyst, Thermal treatment, Gas phase.*

INTRODUCTION

The sol-gel chemistry is a powerful method to obtain catalytic materials with unique morphological and chemical properties [1,2]. Some of the features of these materials are the high surface area and controlled porosity. These compounds allow to incorporation of different elements that highly dispersed through out the matrix [3]. Copper-supported catalysts have been extensively studied for industrial applications [4, 5]. Copper dispersed in micro porous matrices have been attended as catalysts for the selective reduction of nitrogen oxides [6,7] and hydrocarbon combustion [8]. Supported copper catalysts have been attracted due to

* *To whom correspondence should be addressed.*
+ *E-mail: htouhidi@nrcam.org , htouhidi@yahoo.com*
1021-9986/13/3/37 8/$/2.80

recent practical applies in methanol steam reforming [9], dehydrogenation [10] and ester hydrolysis [11]. The preparation method and the nature of the interaction between the support material and the catalytic species are important for deeper understanding of copper-containing catalysts. This is necessary to disperse fine particles in well-defined pores in a support to achieve higher catalytic activity.

There are the interesting and promising processes and catalytic materials developed, from direct decomposition [12,13] to selective reduction processes using ammonia [14,15] as reductants. These systems have high mechanical and hydrothermal stability [16]. Therefore, this is important to further study these systems in order to determine their potential towards the various reactions involving the transformation of nitrogen oxide species [17]. In this investigation, the host matrices were extensively embedded with copper oxide that was produced with one distinct concentration about 10 wt %. The characterization of the catalysts was examined by TGA, TEM, BET and TPR methods at different temperatures [16]. The recent investigation was devoted to the systematic reactivity study of CO & NO oxidation and N_2O decomposition on dispersed copper oxide nano-catalysts into silica supports, in order to determine the ability of these materials to convert carbon oxide and nitrogen oxide into harmless species by different reaction paths. Finally, FT-IR spectra confirm the convert CO, NO oxidation and N_2O decomposition to harmless species, separately.

EXPERIMENTAL SECTOIN

Materials

In this investigation, the raw materials consist of tetraethyl ortho-silicate (TEOS) (Fluka, 98%), ethanol absolute (EtOH) (Merck), copper nitrate tri-hydrated ($Cu(NO_3)_2{\cdot}3H_2O$) (Merck) were used as the initial solution, nitric acid (HNO_3) (Merck, 65%) and acetic acid (CH_3COOH) (Merck, 99-100%) were applied as catalysts, with the mentioned specification.

Sample preparation

Nano-composites were prepared from TEOS (tetraethyl-orthosilicate), ethanol and de-ionized water (DI) in a new total molar ratio of TEOS:ETOH:H_2O=1:4:11.7 with using HNO_3 as catalyst. Copper nitrate tri-hydrated (10 wt %) was added to the starting solution during preparation processing [18]. The samples were prepared in monolithic form, dried at 100 °C for 6 hours, and thermally treated at 200, 400, 600, 800, and 1000 °C at a slow rate 50 °C/h for 2 hours in air. Catalytic activity related to carbon monoxide oxidation was carried out with nano-catalyst with flows of CO and synthetic air controlled by mass flow controllers. Carbon monoxide steady-state conversions were obtained with keeping the catalyst at the reaction temperatures for 2 hours. The reactions were performed in a continuous reaction line equipped with a set of mass flow controllers for the preparation and regulation of the reactant mixture concentration, a tubular vertical electric oven (maximum temperature of 1000 °C), a quartz tubular micro reactor (5 mm i.d.), and analyzers (FT-IR spectrometer from Bio-Rad with DTGS detector) put on the line for the qualitative determination of the fed and vented gaseous species. The mass of catalyst (particles of 2.5-3.5 nm in size) put on the porous septum of the reactor ranged from 35 mg down to 13 mg for total flows of the gaseous mixtures in the 3-6 Nl/h interval, realizing contact times in the 0.36 seconds. Catalytic activity related to nitrogen monoxide oxidation was carried out with nano-catalyst with flows of NO and synthetic air controlled by mass flow controllers. The calcimined samples were pre-treated in O_2/He flow (20 %, v/v) while rising the temperature in stages up to 350 °C and maintained it for 4 hours. The gas mixtures obtained from 1 % NO/He and 10 % O_2/He cylinders were further diluted in He and contained 1500 ppm of NO with an O_2 content in 15000 ppm. Each reaction was studied for different temperatures from 150 to 600 °C. In any case, temperature was regularly increased at step starting from the lowest to the maximum, at rate of 10 °C/min. Each plateau of temperature was maintained for 90 min in order to access of the steady-state conditions [19]. Three studied catalyst in this work, have been prepared with starting from silica supports onto which the CuO phase was doped. The catalysts were synthesized by the sol-gel route as described in ref. [20]. The CuO dispersion was performed by these methods with starting from copper nitrate tri-hydrated precursor. Details on the adopted dispersion methodology can be found in ref [20]. The obtained powders labeled as SG-400, SG-600 and SG-800 were dried at 100 °C for 2 hours and eventually calcimined at 400, 600 , 800, and 1000 °C for 1.5 hours [21]. The main textural properties of the supports and catalysts

are collected at the Table 1. One type of catalytic reaction was realized as detailed in the text. The reactions were performed in a continuous reaction line equipped with a set of mass flow controllers for the preparation and regulation of the reactant mixture concentration. A tubular vertical electric oven (maximum temperature of 1000 °C), a quartz tubular micro reactor (5 mm i.d.), and analyzers (FT-IR spectrometer from Bio-Rad with DTGS detector) put on the line for the qualitative determination of the fed and vented gaseous species. The mass of catalyst (particles of 5 nm in size) put on the porous septum of the reactor ranged from 30 mg down to 10 mg for total flows of the gaseous mixtures in the 3-6 Nl/h interval, realizing contact times in the 0.54 seconds. Catalytic conversion of di-nitrogen oxide (N_2O) was carried out with flows of N_2O and synthetic air controlled by mass flow controllers. The calcimined samples were pre-treated in O_2/He flow (20 %, v/v) while raising the temperature in stages up to 350 °C and maintained it for 4 hours. The gas mixtures obtained from 1 % N_2O/He and 10 % O_2/He cylinders were further diluted in He and contained 1500 ppm of N_2O with an O_2 content in 15000 ppm for the N_2O decomposition reactions. Each reaction was studied for different temperatures realizing in the interval from 150-600 °C. In any case, temperature was regularly increased at step starting from the lowest to the maximum, at flow rating of 10 °C/min. Each plateau of temperature was maintained for 90 minutes in order to access of the steady-state conditions [22].

Characterization

Thermal Gravimetric Analysis (TGA) was obtained by rheometric scientific instrument, model STA 1500.

A Transmission Electron Microscope (TEM) Em208S series, (Phillips Company) operating at 100 kV was used for this investigation. The dry samples were ground and suspended in dry cyclohexane and sonicated for 30 minutes. Then the solutions were allowed to settle and a droplet of the resulting supernatant was placed on a holley carbon film and dried.

The porosities of the samples were analyzed by nitrogen adsorption/desorption measurements fitted to (a BET isotherm) with using an autosorb instrument (Quanta-chrome, Nova 1200). The samples were pre-treated for 3 hours under vacuum at 100 °C (for the sample dried at 100 °C) and at 200 °C (for samples treated at higher temperatures than 100 °C). Gaseous nitrogen was used with a 5 hours adsorption/desorption cycle.

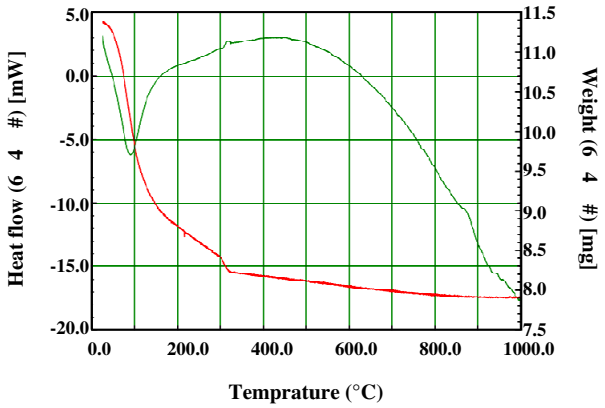

Fig. 1: Thermal analysis of $Cu(NO_3)_2@SiO_2$ nano-composite.

Temperature-Programmed Reduction (TPR) was applied to investigate the ability of copper species for the reaction with gas-phase molecules. The sol-gel samples were used for the TPR directly after the thermal treatment with no pre-activation. For TPR experiments, 20 mg samples in a quartz tube under H_2 (8 %)/N_2 flow were heated at 10 °C. min^{-1} up to 700 °C and the H_2 consumption monitored by a Thermal Conductivity Detector (TCD).

The acidity of solution (pH) was measured by omega pH-meter, model 744.

The condensation and annealing of the samples were performed in a heat furnace with high thermal capacity (1500 ˚C).

RESULTS AND DISCUSSION

Structural analysis

Fig. 1 presents a curve related to the heat flow (mW) and weight (mg) variations to temperature (°C) that is due to thermal analysis of copper oxide on the silica matrix. We can see a high decreasing in heat flow (from 3 to -6 mW). In these temperatures (20-90 °C), the evaporation water and solvent is easy, but at 90-200 °C temperature range and higher to 450 °C, we have a rising at heat flow. In this range, the heat flow rises (from -6.5 to 3 mW) and the reaction is performed hardly and we must use a catalyst in this step [23, 24].

At 450-1000 °C, we have a high reducing at heat flow (from 3 to -17 mW) and the reaction is done easily. Thermal gravimetric curve presents the weight variations to temperature. In related to this, a intense reducing in weight is seen at 30-300 °C, because we miss a high contents water, alcohol, solvent and so on. The nitrate groups have been decomposed that NO_2 gas is formed

Table 1: Thermal treatment effects on the surface area, porosity and density of CuO@Silica.

Sample	T(°C)	Surface area (m^2/g)	Pore radius (Å)	ρ_{pic} (g/cm^3)	V_p (cm^3/g)
CuO100	100	254.0	12.0	0.72	196
CuO400	400	351.0	17.0	0.70	611
CuO600	600	425.1	21.8	0.73	682
CuO800	800	163.0	14.0	074	143
CuO1000	1000	8.0	5.0	0.98	11

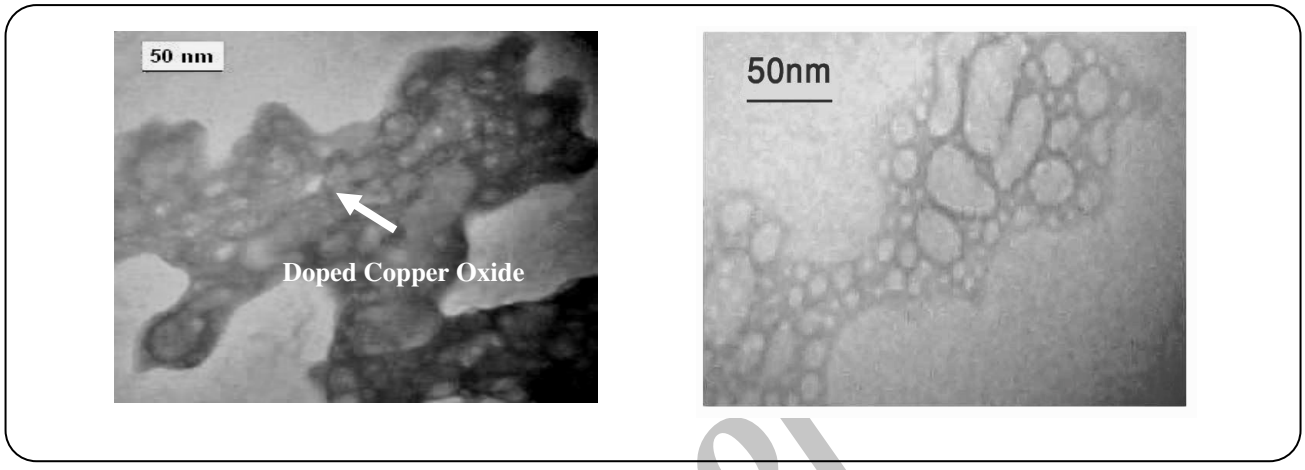

Fig. 2: The TEM micrographs of CuO@SiO_2 nano-composite at (a) 400 °C and (b) un-doped silica matrix.

and we can see a reducing weight (from 11.4 to 8.2 mg) at 320-1000 °C. We also have a slow rate in weight reducing (from 8 to 7.9 mg) that leads to condensation, densification and decomposition steps that are near together, but in all of the thermal analysis steps, a total decreasing is observed in weight (from 11.4 to 3.5 mg).

The microstructure of the xerogel was examined by TEM. Powder samples with 10 wt. % copper after ambient drying and thermal treatment at 400 °C in air for 1 hour were objected to TEM using bright field, and the resulted image was compared with the un-doped silica in Fig. 2. No crystalline species were detected without thermal treatment, and bright field images show a typical amorphous xerogel [24]. These figures confirm the formation of average size of about 50 nm. This process has completely depended on the effects of thermal treatment and copper source. These metallic nano-composites have a structure with excellent stability and reproducibility [25].

The copper ions were doped into silica matrix to copper nitrate form and there are no more copper oxide particles. But with rising temperature and decomposition of copper nitrate, the copper oxide particles were formed and interact with silica matrix by OH groups [20,26]. It has been reported that interaction of support and copper oxide were performed by hydrogen atom with hydroxyl groups [20].

The effects of the thermal treatment on the textural properties of the sol-gel samples were collected at the Table 1. The obtained data were presented that the treatment at 600 °C, produced the largest surface area, pore size radius with the low density. These results indicate the loss of volatile compounds from the porous structure. Once the volatile compounds were eliminated from the network, an increase occurs in the porosity and the gas pore interacts. It is important for the sample treated at 400 °C, which the surface area increases of 38 % (from 254 to 351 m^2/g), whereas the pore volume shows a much more pronounced increase of 211.7 % (from 196 to 611 cm^3/g). For the sample treated at 800 °C, the surface area decreases of 53.5 %, whereas the pore volume shows reduction of 76.6 %. For the sample treated at 1000 °C, a surface area decrement of 95 % was observed, whereas the pore volume shows a reduction of 92.3 % and porosity decrease of 64.3 % (from 14 to 5 Å).

Table 2: TPR of H_2 consumptions for $CuO@SiO_2$.

Treatment temperature (°C)	H_2 consumption (mol/g)	Relative H_2 consumption (%)
100°C	650	100
400°C	650	100
800°C	300	46
1000°C	100	15

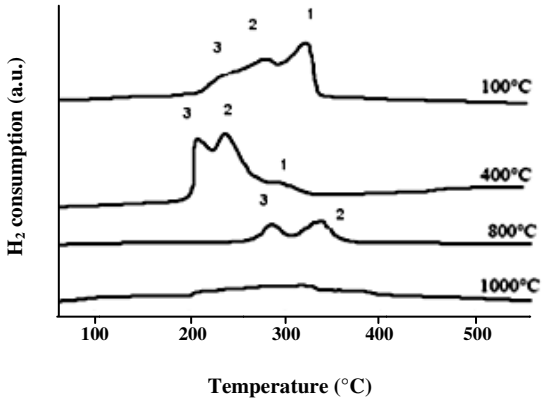

Fig. 3: The TPR profiles of $Cu(NO_3)_2@SiO_2$ samples treated at 100, 400, 800 and 1000 °C.

In authors view, it is related to the size and shape of micro-, meso- and macro-porous, which modify the samples were treated at different temperatures. For the higher temperatures (800 and 1000 °C), the surface area and porosity strongly decrease due to densification process. The results have presented a significant contribution of micro-porous in the material treated at 100 and 400 °C. For higher temperatures, the surface area decreases due to the presence of micro and meso-porous, but the contribution of the meso-porous area in the total surface progressively increases [26]. Thermal Program Reduction (TPR) experiments were shown the reduction of copper species to Cu^0 by H_2. Both Cu^{2+} and Cu^{1+} ions were directly reduced in a single step to form of Cu^0. The TPR analysis of the samples treated at different temperatures were presented in the Fig. 3. The TPR profile of the sample Cu100 presents three hydrogen consumption peaks; a large peak at (1) 325 °C, two minor ones at (2) 280 and (3) 245 °C. For the sample of Cu400, the TPR profile was- shifted at ~25 °C to lower temperatures. The largest peak was observed for the sample Cu400 at (1) 290 °C was much smaller and the other peaks at (2) 255 and (3) 220 °C increase in intensity. These results indicate that the peak (1) is related to the reduction of $Cu(NO_3)_2$ and the peaks (2) and (3) are due to the reduction of copper oxides.

When the sample was treated at 800 °C, TPR profile was shifted back to higher temperatures and peak (1) due to $Cu(NO_3)_2$ was absent, whereas peaks (2) and (3) related to copper oxides, decrease strongly in intensity. At 1000 °C, TPR profiles present that the peaks (2) and (3) were mixed together and form a broad peak.

It can be observed that the hydrogen consumption decreases with rising of temperatures according to the results obtained at the Table 2. The samples annealed at 800 and 1000 °C only have 46 and 15 % of amount of copper species available for reduction, in comparison to the samples annealed at 100 and 400 °C, respectively. These results can be related to the reduction of copper ions by the organic compounds presented in the silica matrix during the thermal treatment. Moreover, all thermal treatments were carried out in air and a reduced copper form such as Cu^0 species. To explain the decrease in TPR of H_2 consumption, one can envisage that treatment at temperatures higher than 800 °C lead to the densification process with sintering and closing of the pores that allow to an entrapment of copper species in the vitreous silica matrix. The entrapped copper species can not be available on the surface for the reaction with H_2 during TPR experiments [27].

The results of catalytic tests for CO oxidation of $CuO@SiO_2$ nano-catalysts treated at different temperatures were displayed in the Fig. 4. It can be seen that sample of CuO-400 presents the largest catalytic activity at 500 °C that CO conversion is about 35 mmol/g.min that followed by CuO-800 (CO conversion; 23 mmol/g.min) and CuO-1000 (CO conversion; 18mmol/g.min) at 500 °C [28]. This trend can be explained by the decrease in surface area, thus the decrease in concentration of copper species available for reactions with molecules from the gas phase.

The catalytic sample treated at 100 °C has both the second largest surface area and surface copper concentration; it presents low catalytic activation (CO conversion; 14 mmol/g.min) at 500 °C. This is probably due to the presence copper nitrate, which is not catalytically active for CO oxidation. The ability to oxidize NO to NO_2 was studied over the three CuO-base catalysts.

The obtained results in terms of NO and NO_2 concentrations as a function of the reaction temperature for an O_2 concentration of 15,000 ppm were reported in the Fig. 5. Very light decrease of the NO reagent was observed for all the catalysts. The NO concentrations passed through a minimum around 400 °C due to a maximum of the NO_2 concentrations, in any case. The NO_2/NO ratios increased from 0.1 to 0.4 values with temperature; once attained 400 °C, the ratios decreased as expected from the equilibrium concentration curve [29].

All the mechanistic interpretations emphasize the need for labile surface oxygen to complete the catalytic cycle by O_2 de-sorption [30,31]. Furthermore, the decomposition was carried out feeding a lean concentration of N_2O reagent and a large amount of O_2. In this oxidizing condition, the copper active sites had to work in their higher oxidation state (Cu^{2+}) and surrounded with oxygen coordination [23]. Fig. 6 reports the N_2O residual concentration profiles and those of N_2O to N_2 conversion as a function of reaction temperature for the three CuO-based catalysts. At each reaction temperature, the N_2O residual concentration was monitored as a function of temperatures to control the attainment of stability conditions. Both at low and high temperatures, the stability were attained by the first 30 minutes of reaction without no loss of activity for higher temperatures. The start up of the reaction can be observed around 450 °C on CuO-400 and CuO-600 and at little higher temperature on CuO-800. The N_2O conversion regularly increased with temperature in the following sequence: CuO-600>CuO-400>CuO-800

At 500 °C, the activity of CuO-600 was four times higher than that of CuO-800 and double of that of CuO-400, while, at higher temperatures (550 °C), the activity of CuO-600>75 % and activity of CuO-400, CuO-800<50 % in this temperature. But at higher temperatures (600 °C), N_2O conversion of CuO-600, CuO-400 was quite similar near to 100 % and activity of CuO-800 is lower of 75 %. N_2O concentration of CuO-400, CuO-600 and CuO-800

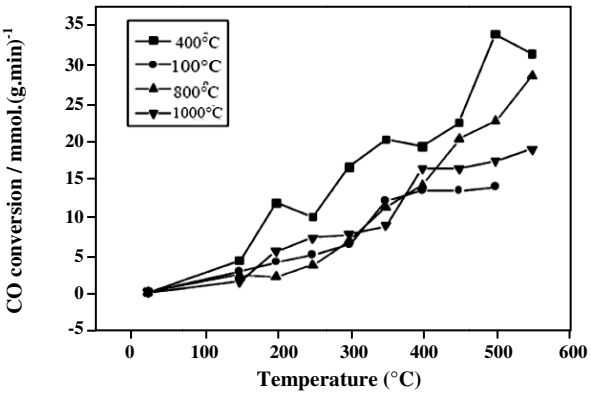

Fig. 4: Catalytic oxidation of carbon monoxide in the presence of CuO@SiO_2.

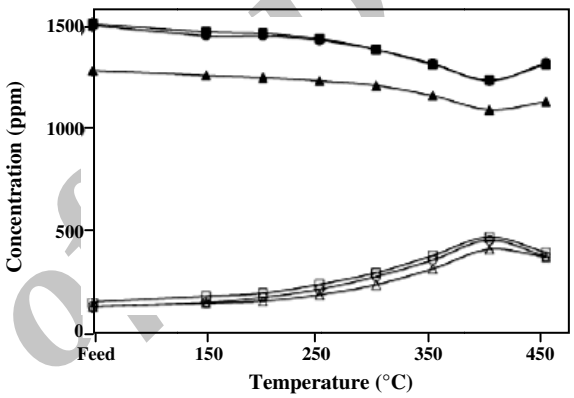

Fig. 5: Oxidation of NO. Profiles of concentration of the reagent (NO, filled symbol) and product (NO_2, open symbol) obtain working with 15,000 ppm O_2 as a function of reaction temperature for the CuO-400 (circle symbol), CuO-600 (triangle symbol) and CuO-800 °C (square symbol).

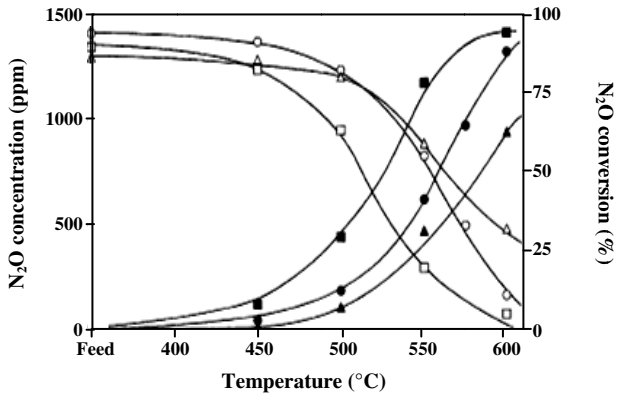

Fig. 6: N_2O decomposition reaction. Profiles of N_2O concentration (open symbols) and N_2O conversion (filled symbols) as a function of reaction temperature for the CuO-400 (circle symbol), CuO-600 (square symbol) and CuO-800 (triangle symbol).

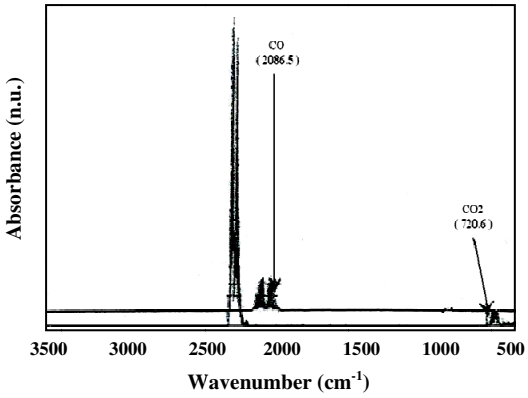

Fig. 7: FTIR spectrum of the C-containing species studied in the various re-activity.

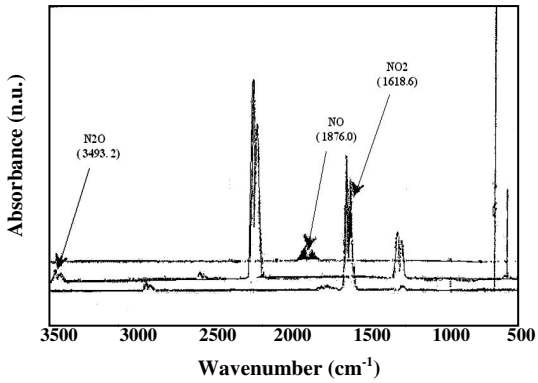

Fig. 8: FTIR spectrum of the N-containing species studied in the various reactions as reactants and/or reaction products.

were compared together in the Fig. 6. The start up of the reaction can be seen around 450 °C for CuO-400, CuO-600 and CuO-800**.** At 500 °C, N_2O concentration of CuO-600 is 1000 ppm while, N_2O concentration CuO-400 and CuO-800 are identical, lower of 1500 ppm. At 550 °C, N_2O concentration of CuO-600 is lower of 500 ppm and N_2O concentrations CuO-400 and CuO-800 are similar of about 1000 ppm. At higher temperature about 600 °C, N_2O concentrations of CuO-400 and CuO-600 decrease intensely, and reach near of zero but N_2O concentrations of CuO-800 is about of 500 ppm.

This data presents, the main activity of three catalysts is at 450-600 °C temperature range. Also, at 550 °C, activity of CuO-600 is very high and we can use the CuO-600 for N_2O decomposition at 550-600 °C. The fed and vented gases from the reactor alternatively flowed through a gas cell (multiple reflection gas cells with 2.4 m path length) in the beam of the FTIR spectrometer. The measurements were carried out at 0.50 cm^{-1} resolution, with accumulation of 19 scans per spectrum. CO (2086.5 cm^{-1}) and CO_2 (720.6 cm^{-1}) for the C-containing species, NO (1876.0 cm^{-1}), N_2O (3493.2 cm^{-1}), and NO_2 (1618.6 cm^{-1}) for the N-containing species were quantified by the intensity of selected absorbance lines in Figs .7 and 8. During the catalyst tests, the total absorbance of all the IR active species flowing from the reactor was monitored each 120 s. For the reactions that lead to the formation of N_2 as product (N_2O-Dec), its concentration was determined by the FTIR analysis, subtracting the sum of all the N-containing species flowed out from the reactor from that of all the N-containing species fed into the reactor.

CONCLUSIONS

The evolution of the copper species moves from copper nitrate to copper oxide species by thermal treatment. After decomposition of the copper nitrate, the copper oxide particles were formed and they interact with the silica matrix via hydroxyl groups. The TEM micrographs confirm the formation of colloidal particles of about 50 nm size for $CuO@SiO_2$ nano-composites at 400 °C. Also, The TPR experiments show the reduction of copper species to Cu^0 by H_2. Both Cu^{2+} and Cu^{+1}ions were reduced directly in a single step to form of Cu^0. Also, these experiments present relation between H_2 consumption and temperature. In the author view, there is a correlation between the existence of copper oxide particles embedded into the silica matrix, and the effects of thermal treatment. These effects might be influenced to the interaction between the guest particles and the matrix host. According to this study, the exact composition of nano-catalyst depends on the annealing temperatures and the choice of appropriate copper source and production method of nano-particles. Also, the results are presented the systematic reactivity study of CO & NO oxidation and N_2O decomposition on dispersed copper oxide nano-catalysts into silica supports, in order to determine the ability of these materials to convert carbon oxide, nitrogen oxide and di-nitrogen oxide into harmless species at different temperatures.

Received : May 2, 2011 ; Accepted : May 6, 2013

REFERENCES

[1] Brinker C.J., Scherer G.W., "Sol-Gel Science", Academic Press, San Diego, CA, p. 908 (1990).

[2] Hench L.L., West J.K., The Sol-Gel Process, *Chem. Rev*. **9,** p**.** 33-72 (1990).

[3] Pajonk G.M., Catalytic Aerogel, *Catal. Today*, **35,** p.319 (1997).

[4] Ulrich, D. R., Prospects for Sol-Gel Process, *J. Non-Cryst. Sol.* **121**, p. 465 (1990).

[5] Fu S.S., Samorijai G.A, Role of Medium-Chain Alcohols in Interfacial Films of Nonionle Microemulsion, *J. Phys. Chem*., **96,** 4542 (1992).

[6] Diaz R., Lazo M.F., Spectroscopic Study of CuO/CoO Catalyst Supported by Si-Al-Y Zeolit Matrices Prepared by Two Sol-Gel Method. *J. Sol-Gel Sci. Technol.,* **17,** p. 137-144 (2000).

[7] Shelef, M., Selective Catalytic Reduction of NO_x with N-Free Reductants, *Chem. Rev*. **95,** p**.** 209 (1995).

[8] Neyestanki A.K., Kumar N., Fluorescence of Flullerene Derivatives at Room Temperature, *Appl. Catal.* **B7,** p. 111 (1995).

[9] Kobayashi H., Takezawa N., Spectroscopic and Thermodynamic Studies of Unsaturated Nitril Compounds, *J. Catal.* **69**, p. 487 (1981).

[10] Sodesawa T., Nagacho M., Copper-Modified Mesoporous MCM-41 Silica: FT-IR and Catalytic Study, *J. Catal.,* **102**, p.460 (1986).

[11] Brands D.S., Poels E.K., Bliek A., Study on Cu-Mn-Si Catalysts for Synthesis of Cyclo-Hexanone., *Appl. Catal.* **A 184,** p. 279 (1999).

[12] Garin F., NO Decomposition over the Electrochemical Cell of Lanthanum Stannate, *Appl. Catal*., **222,** p. 183 (2001).

[13] Liu Z., Amiridis M.D, Chen Y., The Synthesis, Characterization and Catalytic Reaction Studies, *J. Phys. Chem.* **B109**, p. 1251 (2005).

[14] Frozatti P., *Appl. Catal.*, **A 222**, p. 212 (2001).

[15] Koebel M., Madia G., Elsener M., Selective Catalytic Reduction of NO and NO_2 at Low Temperatures *Catal. Today,* **73,** p.239 (2002).

[16] Nobukawa T., Yoshida M., Tomishige K., The Positive Effect of NO on the N_2O Decomposition Activity of Fe-ZSM-5, *J. Catal*., **229,** p. 374 (2005).

[17] Seker E., Gulari E., Hammerle R.H., Lambert C., Leerat J., NO Reduction by Urea Under Lean Conditions Over Alumina Supported *Appl Catal A*., **226,** p. 183 (2002).

[18] Bennici S., Carniti P., Gervasini A., A Study of NO+CO Reaction Over Various Supported Catalyst, *Catal. Lett*., **98**, p. 187 (2004).

[19] Carniti P., Gervasini A., Bennici S., Experimental and Modelisation Approach in the Study of Acid Site Energy Distribution by Base Desorption, *J. Phys. Chem.,* **B109,** p. 1528 (2005).

[20] Tohidi S.H., Grigoryan G.L., Sarkezyan V.A., Ziaie F., Effect of Concentration and Thermal Treatment on the Properties of Sol-Gel Derived CuO/SiO_2 Nanostructure, *Iran. J. Chem. Chem Eng.*, **29**(2), p. 27 (2010).

[21] Tohidi S.H., Novinrooz A.J., Preparation and Study of Molecular Structure of Copper Ions Doped in a Silica Xerogel Matrix, *Int. J. Eng.,* **19,** p. 53 (2006).

[22] Gervasini A., Carniti P., Auroux A., Surface Acidity of Catalytic Solids, *Thermochim. Acta*., **434,** p. 42 (2005).

[23] Gervasini A., Carntti P., Redox Properties in Relation with De-Nox Activity, *Catal Lett.,* **84,** p. 235 (2002).

[24] Tohidi S.H., Grigoryan G.L., Sarkezyan V.A., 6th International Conference on Nanoscience & Nanotechnology, NN09, Thessaloniki, Greece, 94 (2009).

[25] Mohanan J.L., Brock S.L., Sol-Gel Processing of Semiconducting Metal Xerogels, *Chem. Mater.,* **15,** p. 2567 (2003).

[26] Wang Z., Liu Q., YU J., Wu G., Wang A., Surface Structure and Catalytic Behavior of Silica Supported Copper Catalyst Prepared by Impregnation, *Applied Catalysis A.*, **239**, p. 87 (2003).

[27] Martinez J.R., Ruiz F., Vorbiev Y.V., Gonzalez-Hernandez J.F., Prez-Robles J., Gonzalez-Hernandez, Maepo Structural de Silica Xerogel Utilizando Espectroscopia, *J. Chem. Phys.* **109**, p. 575-581 (1998).

[28] Ruiz F., Martinez J.R., Gonzalez-Hernandez, Formation of Silicate Structures in Cu-containing Silica, *J. Mater. Res.* **15**, p. 2875-2879 (2000).

[29] Yang Kim M., Catalytic Reduction of N_2O by H_2 over Well Characterized Pt Ssurfaces; *Korean J. Chem. Eng.*, **23**, p. 90818 (2006).

[30] Chang K.S., Song H., Park Y.S., Woo, Preparation of Fatty Acid Methyl Esters for Gas Chromatography, *Appl. Cata*l. **A 273,** 223 (2004).

[31] Dandekar A., Vannice M.A., *Appl. Catal.* **B 22**, p. 179 (1999).